Large Proximity-Induced Spin Lifetime Anisotropy in Transition-Metal Dichalcogenide/Graphene Heterostructures

Ghiasi, Talieh Sadat; Ingla Aynés, Josep; Kaverzin, Alexey; van Wees, Bart

Published in:
Nano Letters

DOI:
10.1021/acs.nanolett.7b03460

Publication date:
2017

NANO LETTERS

Letter

Cite This: Nano Lett. 2017, 17, 7528−7532

pubs.acs.org/NanoLett

Large Proximity-Induced Spin Lifetime Anisotropy in Transition-Metal Dichalcogenide/Graphene Heterostructures

Talieh S. Ghiasi,* Josep Ingla-Aynés, Alexey A. Kaverzin, and Bart J. van Wees

Physics of Nanodevices, Zernike Institute for Advanced Materials, University of Groningen, Groningen, 9747 AG, The Netherlands

Supporting Information

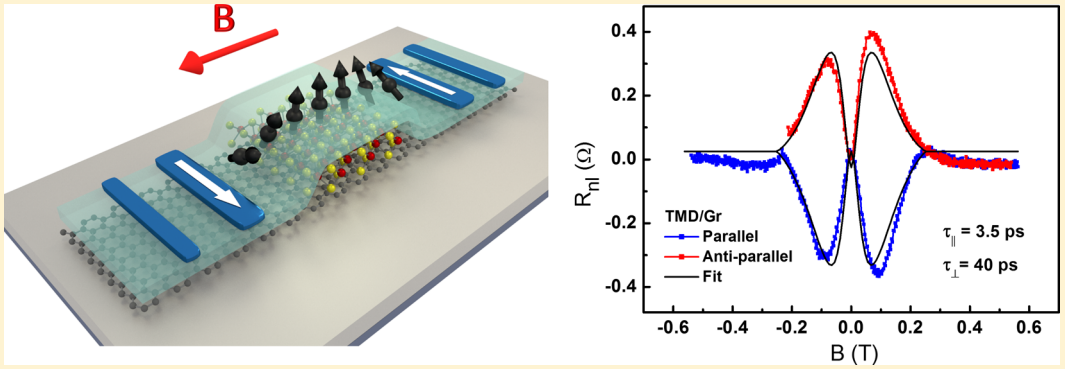

ABSTRACT: Van der Waals heterostructures have become a paradigm for designing new materials and devices in which specific functionalities can be tailored by combining the properties of the individual 2D layers. A single layer of transition-metal dichalcogenide (TMD) is an excellent complement to graphene (Gr) because the high quality of charge and spin transport in Gr is enriched with the large spin−orbit coupling of the TMD via the proximity effect. The controllable spin-valley coupling makes these heterostructures particularly attractive for spintronic and opto-valleytronic applications. In this work, we study spin precession in a monolayer $MoSe_2$/Gr heterostructure and observe an unconventional, dramatic modulation of the spin signal, showing 1 order of magnitude longer lifetime of out-of-plane spins compared to that of in-plane spins ($\tau_{\perp} \approx 40$ ps and $\tau_{\parallel} \approx 3.5$ ps). This demonstration of a large spin lifetime anisotropy in TMD/Gr heterostructures, is a direct evidence of induced spin-valley coupling in Gr and provides an accessible route for manipulation of spin dynamics in Gr, interfaced with TMDs.

KEYWORDS: *Spintronics, graphene, transition-metal dichalcogenide, spin-valley coupling*

Graphene, with its high charge-carrier mobility and weak spin−orbit coupling (SOC), is an excellent host for long-distance spin transport.[1−4] However, data storage and information processing in spin-based devices require active control of the spin degree of freedom.[5] Therefore, manipulation of the spin currents, i.e., tuning spin polarization and spin lifetime, has been a topic of recent theoretical[6−9] and experimental[10−17] research. To fulfill this goal, one of the main approaches is fabrication of hybrid devices, in which the properties of the 2D building blocks complement each other.[18,19] The strong SOC of TMDs, orders of magnitude larger than the one of Gr,[20] can modulate the spin dynamics in the Gr channel, while the high quality of charge transport of Gr is preserved.[11] The induced SOC in Gr via proximity effect of a TMD can be in the order of 10 meV,[7] experimentally confirmed by the observation of weak antilocalization[12−14] and spin Hall effect[15] in these heterostructures, and by the suppression of the spin lifetimes[16,17] to less than a few picoseconds.

The modulation of spin currents in bulk TMD/Gr van der Waals heterostructures has been already reported[10,16] based on gate-controlled spin absorption by the TMD. Moreover, the spin-valley locking has been used for optical excitation of spins[21,22] in TMDs, which are injected into and transported by the underlying Gr. However, in this work we study how the spin transport properties of Gr are influenced by the proximity of monolayer TMDs. We address the induced anisotropic nature of spin relaxation in these hybrids, originating from the strongly coupled spin and valley degrees of freedom.[23] Our results, consistent with the theoretical predictions,[8] give an insight into the valley-coupled spin dynamics in TMD/Gr heterostructures and are very relevant to acquire a complete understanding of the physics of (opto-) valleytronics and spintronics in these systems.

We fabricate devices based on a vdW heterostructure of monolayer $MoSe_2$/monolayer Gr, covered with an hBN bilayer (Figure 1). These atomically thin layers are exfoliated from their bulk crystals and are stacked by a dry pick-up technique[24] that provides high-quality and polymer-free interfaces. To study spin transport, we use ferromagnetic cobalt contacts using the

Received: August 13, 2017
Revised: October 24, 2017
Published: November 27, 2017

DOI: 10.1021/acs.nanolett.7b03460
Nano Lett. 2017, 17, 7528−7532

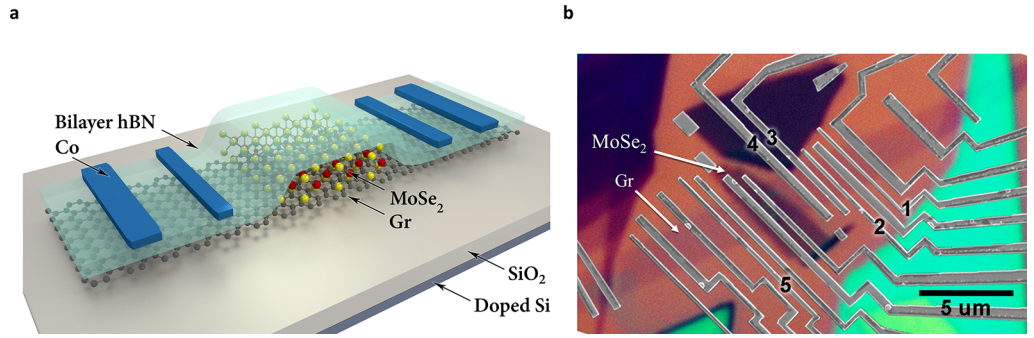

Figure 1. Device geometry. (a) Sketch of the $MoSe_2$/Gr van der Waals heterostructure on a SiO_2/Si substrate with a top layer of bilayer hBN used as a tunnel barrier for spin injection and detection in Gr with Co contacts. (b) Combination of an optical microscope (OM) image of the van der Waals heterostructure and an SEM image of the Co contacts. The green flake is bulk hBN. The used electrodes for measurements are numbered. The width of the Gr channel is about 2.4 μm.

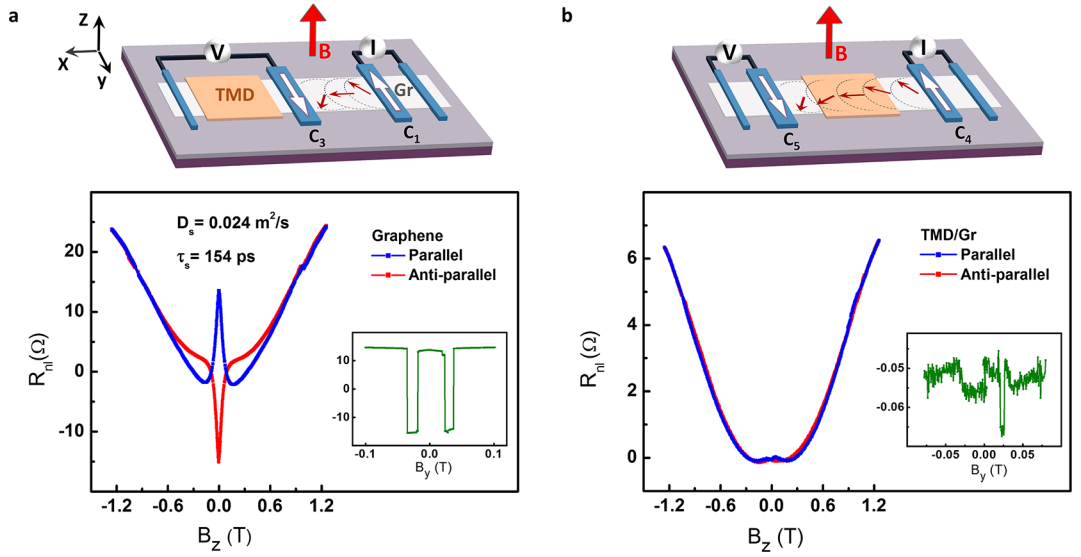

Figure 2. Comparison of Hanle precession measurements with out-of-plane magnetic field (B_z). The device sketches with nonlocal measurement geometries are illustrated (contacts are numbered according to Figure 1b). Nonlocal magnetoresistance (R_{nl}) as a function of B_z and the corresponding nonlocal spin-valve (shown in the inset) are measured (a) on the Gr channel (length: 2.1 μm) with C_1 as the spin injector and C_3 as the detector and (b) across the TMD/Gr region with C_4 as the spin injector and C_5 as the detector (channel length is 4.1 μm, covered with 2 μm of $MoSe_2$). In our measurement setup, B_z is limited to 1.2 T, which is not sufficient for complete out-of-plane saturation of the contact magnetization. Therefore, the reported magnitude for the out-of-plane spin signal is the lower bound of the real value.

bilayer hBN as a tunnel barrier that allows for highly efficient electrical spin injection and detection.[25]

The conventional four-terminal nonlocal geometry[26] for injection and detection of pure spin currents is shown in Figure 2a. We measure the nonlocal resistance ($R_{nl} = V/I$) while sweeping the magnetic field (B_y) along the easy axis of the Co contacts. All the measurements are carried out at 75 K. The spin-valve signal is defined as the difference in R_{nl}, measured in parallel and antiparallel magnetization configurations of the contacts ($\Delta R_{nl} = R_p - R_{ap}$). The ΔR_{nl} signal of 30 Ω is measured over 2.1 μm of the Gr channel. When an out-of-plane magnetic field (B_z) is applied, the spins undergo Larmor precession in the x–y plane while diffusing. By measuring R_{nl} as a function of B_z, we acquire the so-called Hanle precession curves. The spin lifetime (τ_s), diffusion coefficient (D_s), and contact polarization (~40%) are obtained by fitting the Hanle curves to the solution of Bloch equations.[27] Interestingly, increasing B_z beyond the typical fields sufficient for significant spin dephasing enhances R_{nl} over its value at $B = 0$ T. This increase in the spin signal is attributed to the contribution of the out-of-plane spins when the magnetization of the Co electrodes gets pulled out of the graphene plane. We observe that the ratio of the spin signal at high B_z (dominated by the out-of-plane spins) over the in-plane spin signal (at $B_z = 0$ T) increases as the inner detector contact approaches the TMD/Gr region (see section S5.1 of the Supporting Information). This observation is attributed to the fact that in the diffusive Gr channel the presence of the TMD/Gr region influences the spin diffusion in the full channel. The TMD/Gr region plays role as an in-plane spin sink, such that the in-plane spins have shorter lifetime and therefore faster relaxation of them will lead to the detection of smaller in-plane spin signal as compared to that of the out-of-plane spins.

To further understand the effect of the monolayer $MoSe_2$ on spin transport in Gr, we measure R_{nl} across the TMD/Gr region. In Figure 2b, the spin-valve measurement shows a considerable suppression of the in-plane spin signal to ≈15 mΩ, which is about 300 times smaller than the in-plane spin signal in pristine Gr with the same channel length. When we apply B_z and the z-component of the magnetization of the

DOI: 10.1021/acs.nanolett.7b03460
Nano Lett. 2017, 17, 7528−7532

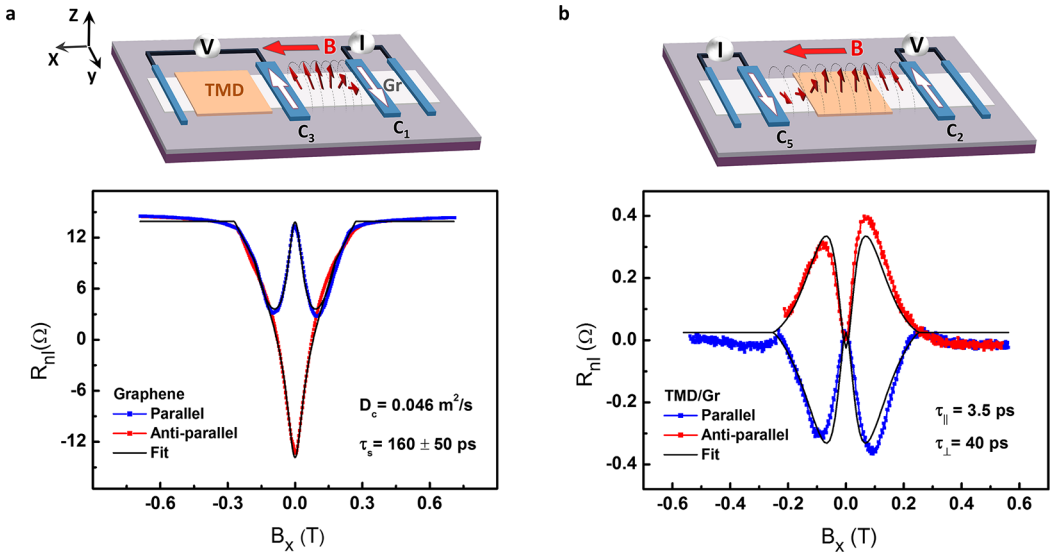

Figure 3. Comparison of Hanle precession measurements with in-plane magnetic field (B_x). The device sketches with nonlocal measurement geometries are illustrated (contacts are numbered according to Figure 1b). R_{nl} as a function of B_x is measured (a) on the Gr channel, fitted with the uniform model (spin injector is C_1 and detector is C_3) and (b) across the TMD/Gr region, with a fit by the four-region model (spin injector is C_5, and detector is C_2) (channel length is 5.6 μm and is covered with 2 μm of $MoSe_2$). The fit to the data is obtained for $\tau_{||}$ = 3.5 ps and $\tau_{\perp}$ = 40 ps. See the Supporting Information for details of the uniform and four-region models.

Co contacts increases, we observe that R_{nl} enhances dramatically to values over 6 Ω. Similar behavior is also observed in the measurements done at 5 K. This observation implies that the out-of-plane spin signal exceeds the in-plane signal by about 3 orders of magnitude. Such a giant contrast between the in- and out-of-plane spin signal can only be understood if the in-plane spin lifetime in the TMD/Gr heterostructure is shorter than 3.5 ps, 2 orders of magnitude smaller than that of the pristine Gr channel (see section S5.2 of the Supporting Information).

To get more information regarding the lifetimes of in-plane spins ($\tau_{||}$) and out-of-plane spins ($\tau_{\perp}$), we apply an in-plane magnetic field (B_x). This direction of magnetic field makes the spins precess in the $y-z$ plane, thus probing both $\tau_{||}$ and $\tau_{\perp}$.[28] By measuring R_{nl} in the pristine Gr regions, we obtain the Hanle precession curves in Figure 3a. As expected, the in-plane spin-signal has its highest value at B = 0 T and decreases when the spins precess. Sufficiently large B_x aligns the Co electrode magnetization in the x direction (saturating at $B_x \approx 0.3$ T), and therefore, the spin signal is restored to its initial value (at B = 0 T). The behavior of the contacts is explained by using the Wohlfarth−Stoner model.[29] The spin transport parameters can be extracted by the fit to the solutions of the Bloch equations,[27] which confirms the isotropic spin relaxation in the Gr region (see section S5.3 in the Supporting Information).

However, when we measure B_x-induced Hanle precession across the TMD/Gr region, we observe a dramatically different behavior (Figure 3b). At B = 0 T, the value of R_{nl} is small and is caused by the in-plane spin transport. As B_x increases, the in-plane spins start to precess in the $y-z$ plane, which generates out-of-plane spins that have longer lifetime. Therefore, the R_{nl} considerably increases in magnitude to about 35 times larger values (at $B_x \approx 0.1$ T) and reverses sign. Beyond 0.1 T the signal decreases due to both the spin dephasing and the saturation of contact magnetization, recovering the in-plane spin signal. This observation is again a direct proof of anisotropic spin-transport in TMD/Gr heterostructure. Using the Bloch equations (eq 1), we can fit the data to an anisotropic relaxation model,[30] accounting for the difference between $\tau_{||}$ and $\tau_{\perp}$ in the TMD/Gr region (see section S5.4 of the Supporting Information):

$$
\begin{aligned}
D_s\frac{d^2\mu_{sx}}{dx^2} - \frac{\mu_{sx}}{\tau_{||}} + \gamma B_y\mu_{sz} - \gamma B_z\mu_{sy} &= 0\\
D_s\frac{d^2\mu_{sy}}{dx^2} - \frac{\mu_{sy}}{\tau_{||}} + \gamma B_z\mu_{sx} - \gamma B_x\mu_{sz} &= 0\\
D_s\frac{d^2\mu_{sz}}{dx^2} - \frac{\mu_{sz}}{\tau_{\perp}} + \gamma B_x\mu_{sy} - \gamma B_y\mu_{sx} &= 0
\end{aligned}
\qquad (1)
$$

where μ_{sx}, μ_{sy} and μ_{sz} are the accumulations of spins with x, y and z directions, respectively and γB is the Larmor frequency. A fit to the data is obtained with values of $\tau_{||}$ = 3.5 ps and $\tau_{\perp}$ = 40 ps, confirming the large spin lifetime anisotropy in the Gr induced by the monolayer $MoSe_2$. The measurements (shown in Figure 3) are carried out at zero gate voltage (V_g), with carrier densities of 4.5×10^{12} cm^{-2} and 1.8×10^{12} cm^{-2} in the pristine Gr and TMD/Gr regions, respectively. With the change of V_g (to ±40 V), we do not see any considerable change in the anisotropy, indicating that the spin absorption cannot be the dominant mechanism for spin-relaxation in TMD/Gr region (see section S6 of the Supporting Information). However, at room temperature (RT), the spin signal in these measurements is below the noise level (0.03 Ω). This can be attributed to the fact that the interfacial spin resistance in TMD/Gr considerably decreases at RT, and therefore, the spins are absorbed by TMD.

According to the recent theoretical predictions,[8] the dynamics of spin transport in Gr in proximity of a TMD are governed by the Dyakonov−Perel (DP) mechanism, which plays a major role in systems with broken inversion symmetry. In a TMD/Gr heterostructure, the strong spin-valley coupling of the TMD is imprinted onto the Gr channel and controls the dynamics of the in-plane spins. The in-plane spin relaxation is

DOI: 10.1021/acs.nanolett.7b03460
Nano Lett. 2017, 17, 7528−7532

affected by both intervalley and momentum scattering, but the former is dominant ($\tau_{\parallel} \propto 1/\tau_{iv}$, with τ_{iv} being the intervalley scattering time). In contrast, the out-of-plane spin relaxation is mainly controlled by the momentum scattering in this system ($\tau_{\perp} \propto 1/\tau_{p}$, with τ_{p} the momentum relaxation time). The spin lifetime anisotropy can be calculated by:

$$\frac{\tau_{\perp}}{\tau_{\parallel}} = \left(\frac{\lambda_{VZ}}{\lambda_{R}}\right)^{2} \frac{\tau_{iv}}{\tau_{p}} + \frac{1}{2} \quad (2)$$

where λ_{VZ} and λ_{R} are the valley Zeeman and Rashba spin−orbit coupling constants, respectively.[8] These terms have been calculated by first-principles as λ_{VZ} = −0.175 meV and λ_{R} = 0.26 meV for a $MoSe_2$/Gr heterostructure.[7] Our experimental observation of spin lifetime anisotropy estimated as $\tau_{\perp}/\tau_{\parallel} \approx 11$, corresponds to an intervalley scattering time of $\tau_{iv} \approx 24$ and $\tau_{p} \approx 2$ ps (with τ_{p} = 0.076 ps). This value matches well with the reported range for τ_{iv} in Gr, extracted from weak localization measurements.[12,31] Note that the exact values of λ_{VZ} and λ_{R} will depend on the TMD−Gr interface, which might result in variation of the relaxation times. However, we believe that the anisotropy as expressed in eq 2 will be less sensitive to the interfacial inhomogeneities.

In conclusion, we have reported the first direct observation of the spin lifetime anisotropy in a TMD/Gr heterostructure, consistent with the theoretical predictions of the TMD SO-induced proximity effects in Gr.[8] The estimated out-of-plane spin relaxation time is 1 order of magnitude larger than that of the in-plane spins. This result is explained by considering the dominant role of the intervalley scattering in the relaxation of the in-plane spins. The effect is attributed to the spin-valley coupling in TMD/Gr as a consequence of the strong spin−orbit coupling in the TMD, the significant wave function overlap between Gr and the TMD, and the associated inversion symmetry breaking. We have demonstrated that the manipulation of spin-transport in the Gr channel is possible by controlled stacking of atomically thin building blocks, such that unprecedented insights into the nature of the spin−orbit interactions are provided by a simple and novel approach in the spin-precession experiments.

Note. After the submission of the present manuscript, we became aware of a related work studying the spin relaxation anisotropy in multilayer WS_2/Gr and MoS_2/Gr heterostructures.[32]

■ ASSOCIATED CONTENT

Supporting Information

The Supporting Information is available free of charge on the ACS Publications website at DOI: 10.1021/acs.nanolett.7b03460.

Additional details on device fabrication, AFM characterization of the vdW heterostructure, charge transport, local magnetoresistance, derivation of the models used for extraction of the spin transport parameters, gate dependence of the spin signal in monolayer $MoSe_2$/Gr heterostructure, and anisotropic spin transport measurements on a monolayer WSe_2/Gr heterostructure. (PDF)

■ AUTHOR INFORMATION

Corresponding Author

*E-mail: t.s.ghiasi@rug.nl.

ORCID

Talieh S. Ghiasi: 0000-0002-3490-5356

Notes

The authors declare no competing financial interest.

■ ACKNOWLEDGMENTS

We kindly acknowledge S. Roche, J. Fabian, G. E. W. Bauer, and A. W. Cummings for insightful discussions. We thank T. J. Schouten, H. M. de Roosz, J. G. Holstein, and H. Adema for technical support. We also acknowledge J. Peiro and M. Gurram for their assistance. This research has received funding from the Dutch Foundation for Fundamental Research on Matter (FOM) as a part of The Netherlands Organisation for Scientific Research (NWO), FLAG-ERA (15FLAG01-2), the People Programme (Marie Curie Actions) of the European Union's Seventh Framework Programme FP7/2007-2013 under REA grant agreement no. 607904-13 Spinograph, the European Union's Horizon 2020 research and innovation programme under grant agreement no. 696656 Graphene Flagship, and supported by NanoLab NL.

■ REFERENCES

(1) Han, W.; Kawakami, R. K.; Gmitra, M.; Fabian, J. *Nat. Nanotechnol.* **2014**, *9*, 794−807.
(2) Roche, S.; et al. *2D Mater.* **2015**, *2*, 030202.
(3) Drögeler, M.; Franzen, C.; Volmer, F.; Pohlmann, T.; Banszerus, L.; Wolter, M.; Watanabe, K.; Taniguchi, T.; Stampfer, C.; Beschoten, B. *Nano Lett.* **2016**, *16*, 3533−3539.
(4) Ingla-Aynés, J.; Meijerink, R. J.; van Wees, B. J. *Nano Lett.* **2016**, *16*, 4825−4830.
(5) Žutić, I.; Fabian, J.; Das Sarma, S. *Rev. Mod. Phys.* **2004**, *76*, 323−410.
(6) Gmitra, M.; Fabian, J. *Phys. Rev. B: Condens. Matter Mater. Phys.* **2015**, *92*, 155403.
(7) Gmitra, M.; Kochan, D.; Högl, P.; Fabian, J. *Phys. Rev. B: Condens. Matter Mater. Phys.* **2016**, *93*, 155104.
(8) Cummings, A. W.; García, J. H.; Fabian, J.; Roche, S. *Phys. Rev. Lett.* **2017**, *119*, 206601.
(9) García, J. H.; Cummings, A. W.; Roche, S. *Nano Lett.* **2017**, *17*, 5078−5083.
(10) Yan, W.; Txoperena, O.; Llopis, R.; Dery, H.; Hueso, L. E.; Casanova, F. *Nat. Commun.* **2016**, *7*, 13372.
(11) Avsar, A.; Tan, J. Y.; Taychatanapat, T.; Balakrishnan, J.; Koon, G.; Yeo, Y.; Lahiri, J.; Carvalho, A.; Rodin, A. S.; O'Farrell, E.; Eda, G.; Castro Neto, A. H.; Özyilmaz, B. *Nat. Commun.* **2014**, *5*, 4875.
(12) Wang, Z.; Ki, D.; Chen, H.; Berger, H.; MacDonald, A. H.; Morpurgo, A. F. *Nat. Commun.* **2015**, *6*, 8339.
(13) Wang, Z.; Ki, D.-K.; Khoo, J. Y.; Mauro, D.; Berger, H.; Levitov, L. S.; Morpurgo, A. F. *Phys. Rev. X* **2016**, *6*, 041020.
(14) Yang, B.; Tu, M.-F.; Kim, J.; Wu, Y.; Wang, H.; Alicea, J.; Wu, R.; Bockrath, M.; Shi, J. *2D Mater.* **2016**, *3*, 031012.
(15) Note that there are some uncertainties in the observation of spin Hall effect[11] due to the complex interpretation of the nonlocal Hall bar measurements, see refs 33 and 34.
(16) Dankert, A.; Dash, S. P. *Nat. Commun.* **2017**, *8*, 16093.
(17) Omar, S.; van Wees, B. J. *Phys. Rev. B: Condens. Matter Mater. Phys.* **2017**, *95*, 081404.
(18) Geim, A. K.; Grigorieva, I. V. *Nature* **2013**, *499*, 419−425.
(19) Novoselov, K. S.; Mishchenko, A.; Carvalho, A.; Castro Neto, A. H. *Science* **2016**, *353*.aac943910.1126/science.aac9439
(20) Kośmider, K.; González, J. W.; Fernández-Rossier, J. *Phys. Rev. B: Condens. Matter Mater. Phys.* **2013**, *88*, 245436.
(21) Luo, Y. K.; Xu, J.; Zhu, T.; Wu, G.; McCormick, E. J.; Zhan, W.; Neupane, M. R.; Kawakami, R. K. *Nano Lett.* **2017**, *17*, 3877−3883.
(22) Avsar, A.; Unuchek, D.; Liu, J.; Sanchez, O. L.; Watanabe, K.; Taniguchi, T.; Özyilmaz, B.; Kis, A. *ACS Nano* **2017**, *11*, 11678.

DOI: 10.1021/acs.nanolett.7b03460
Nano Lett. 2017, 17, 7528−7532

(23) Xiao, D.; Liu, G.-B.; Feng, W.; Xu, X.; Yao, W. *Phys. Rev. Lett.* **2012**, *108*, 196802.
(24) Zomer, P. J.; Guimarães, M. H. D.; Brant, J. C.; Tombros, N.; van Wees, B. J. *Appl. Phys. Lett.* **2014**, *105*, 013101.
(25) Gurram, M.; Omar, S.; van Wees, B. J. *Nat. Commun.* **2017**, *8*, 1.
(26) Tombros, N.; Jozsa, C.; Popinciuc, M.; Jonkman, H. T.; van Wees, B. J. *Nature* **2007**, *448*, 571−574.
(27) Fabian, J.; Matos-Abiague, A.; Ertler, C.; Stano, P.; Žutić, I. *Acta Phys. Slovaca* **2007**, *57*, 565−907.
(28) Raes, B.; Scheerder, J. E.; Costache, M. V.; Bonell, F.; Sierra, J. F.; Cuppens, J.; Van de Vondel, J.; Valenzuela, S. O. *Nat. Commun.* **2016**, *7*, 11444.
(29) Stoner, E. C.; Wohlfarth, E. P. *Philos. Trans. R. Soc., A* **1948**, *240*, 599−642.
(30) Raes, B.; Cummings, A. W.; Bonell, F.; Costache, M. V.; Sierra, J. F.; Roche, S.; Valenzuela, S. O. *Phys. Rev. B: Condens. Matter Mater. Phys.* **2017**, *95*, 085403.
(31) Tikhonenko, F. V.; Horsell, D. W.; Gorbachev, R. V.; Savchenko, A. K. *Phys. Rev. Lett.* **2008**, *100*, 056802.
(32) Benitez, L.; Sierra, J.; Torres, W. S.; Arrighi, A.; Bonell, F.; Costache, M.; Valenzuela, S. *arXiv:1710.11568*. arXiv.org e-Print archive. 2017.
(33) Kaverzin, A.; van Wees, B. *Phys. Rev. B: Condens. Matter Mater. Phys.* **2015**, *91*, 165412.
(34) Ribeiro, M.; Power, S. R.; Roche, S.; Hueso, L.; Casanova, F. *arXiv:1706.02539*. arXiv.org e-Print archive, 2017, accesssed 11-28-2017.

DOI: 10.1021/acs.nanolett.7b03460
Nano Lett. 2017, 17, 7528−7532